FT-IR study of the reaction mechanisms for photocatalytic reduction of NO with CO promoted by various single-site photocatalysts

FT-IR study of the reaction mechanisms for photocatalytic reduction of NO with CO promoted by various single-site photocatalysts

TakashiToyaoa

JunMorishimaa

MasakazuSaitoa

YuHoriuchia

TakashiKamegawab

GianmarioMartrac

SalvatoreColucciac

MasayaMatsuokaa

MasakazuAnpoa

a

Department of Applied Chemistry, Graduate School of Engineering, Osaka Prefecture University, 1-1 Gakuen-cho, Naka-ku, Sakai, Osaka 599-8531, Japan

b

Division of Materials and Manufacturing Science, Graduate School of Engineering, Osaka University, 2-1 Yamada-oka, Suita, Osaka 565-0817, Japan

c

Dipartimento di Chimica IFM, Universita di Torino, Via P. Giuria 7, 10125 Torino, Italy

1. Introduction

Photocatalysis has been widely studied with the aim of developing technologies for the efficient elimination of environmentally undesired chemical substances from air and water [1–4]. Titanium dioxide (TiO_2) is one semiconductor material that has been proven to be effective for the promotion of various photocatalytic reactions, such as water splitting into hydrogen and oxygen [5–7], the decomposition of NOx in air [8,9], degradation of toxic organic impurities in water [10–12], and the removal of volatile organic compounds (VOCs) from the environment [13,14].

In recent years, isolated metal oxides that are highly dispersed in an isolated state within catalyst supports, which are referred to as single-site photocatalysts, have attracted significant attention owing to their efficient and selective photocatalytic properties, which cannot be attained by using bulk semiconductor photocatalysts [15–17]. Metal oxides ($[M^{n+}O^{2-}]$) existing in an isolated state are electronically excited by UV-light irradiation to form the corresponding charge-transfer-excited triplet states ($[M^{(n-1)+}O^{-}]^*$) through one electron transfer from an oxygen atom in ligands (O^{2-}) to the central metal (M^{n+}). In the charge-transfer-excited triplet states, $M^{(n-1)+}$ and O^- pairs can be considered as electron–hole pair states which are localized quite near to each other as compared to the electron and hole produced by irradiation of semiconductor materials. This characteristic feature of metal oxide in isolated states is responsible for a variety of unique photocatalytic reactions, including photo-induced metathesis [18], direct decomposition of NO into N_2 and O_2[19], partial oxidation of hydrocarbons to form oxygen-containing compounds [20], and selective oxidation of CO in the presence of H_2[21]. More recently, we have demonstrated that highly dispersed Mo oxides incorporated within SiO_2 (Mo/SiO_2) are highly active catalysts for UV-light induced reduction of nitrogen oxides, such as NO and N_2O, with CO [22]. Nitrogen oxides are especially harmful atmospheric pollutants, which serve as the cause of acid rain, high local ozone concentrations and photochemical smog, and CO is one of the main toxic gaseous pollutants emanating from automobile exhaust [23–25]. Compared to typical noble metal-containing catalysts, which operate only under high temperature conditions [26,27], single-site photocatalysts have various beneficial features in terms of reduced cost and environmental friendliness. Specifically, processes promoted by these types of cheap transition metal catalysts lead to the simultaneous decomposition of nitrogen oxides and CO under UV-light irradiation at ambient temperatures. As a consequence of their important properties, an understanding of the mechanisms for reactions occurring on single-site photocatalysts is critically important in order to enhance photocatalytic activities and selectivities.

In the study described below, highly dispersed transition metal oxides incorporated within SiO_2 (M/SiO_2: MMo, V, and Cr), serving as single-site photocatalysts, have been prepared by using a facile impregnation method. The activities of these photocatalysts in the promotion of NO reduction in the presence of CO have been investigated. Observations made in an in situ Fourier transform infrared (FT-IR) study have led to a proposed reaction mechanism for this process.

2. Experimental

2.1. Preparation of various single-site photocatalysts

Mo, V, and Cr/SiO_2 (metal content; 0.38 atomic%) were prepared from aqueous solutions of $(NH_4)6Mo_7O_{24}\cdot 4H_2O$, NH_4VO_3, and $Cr(NO_3)_3\cdot 9H_2O$, respectively, by using an impregnation method. The metal–oxide precursors were dissolved in 100 mL of ion-exchange water, and 2.0 g of SiO_2 was then added to the aqueous solutions. The resulting suspensions were stirred at 323 K for 1 h and evaporated to dryness, giving residues that were dried at 373 K in air for 12 h and calcined at 873 K for 8 h.

2.2. Characterization

XAFS (X-ray absorption fine structure) spectra were recorded at the BL-10B and BL-7C facilities of the Photon Factory at the High Energy Accelerator Research Organization (KEK-PF) in Tsukuba. Typically, the Mo K-edge XAFS spectra were measured in the transmission mode, and the V and Cr K-edge XAFS spectra were measured in the fluorescence mode, with a Si(1 1 1) double-crystal monochromator at room temperature. Curve-fitting analyses of the EXAFS (extended X-ray absorption fine structure) spectra were conducted on k3χ (k) in k-space (k range = 3–12 Å−1) using a REX2000J program (Rigaku). The diffuse reflectance UV–vis spectra were recorded with a Shimadzu UV-2200A double-beam digital spectrophotometer at room temperature. The photoluminescence spectra were recorded at room temperature by utilizing a SPEX Fluorolog-3 spectrofluorometer with a quartz cell directly connected to a vacuum line containing stopcocks to allow gas addition and degassing. FT-IR measurements were carried out in the transmission mode using a FT-IR spectrometer (JASCO FT-IR 660 Plus) at room temperature. Self-supporting pellets of the samples were loaded in a specially constructed IR cell, which was equipped with CaF2 windows and directly connected to a vacuum line containing stopcocks to allow gas addition and degassing.

2.3. Photocatalytic reaction

Photocatalytic reactions were carried out with catalysts (100 mg) in a flat bottomed quartz cell at 293 K (closed system) under UV-light irradiation. Prior to each photocatalytic reaction, the catalysts were calcined in O2 (>2.66 kPa) at 773 K for 1 h and then degassed at 473 K for 1 h. NO (28 μmol) and CO (28 μmol) were then added to the cell. UV-light irradiation, employing a high-pressure Hg lamp (Toshiba SHL-100UVQ-2), took place through a water filter in order to avoid heating effects. Reaction products were analyzed by using a gas chromatograph (Shimadzu GC-14B with a thermal conductivity detector) equipped with a porapak Q column.

3. Results and discussion

3.1. Characterizations of M/SiO2 (MMo, V, and Cr)

XAFS measurements were carried out in order to elucidate the local structure of the transition metal oxide components within M/SiO2 (MMo, V, and Cr). Fig. 1A shows the Mo K-edge XANES (X-ray absorption near-edge fine structure) spectrum of Mo/SiO2, whose shape is similar to that of Na2MoO4 (data not shown) employed as a reference sample with tetrahedral coordination [28]. The characteristic feature of the XANES spectrum of Mo/SiO2 is the existence of a pre-edge peak corresponding to the 1s–4d transition of the Mo6+-oxide [29]. Additionally, as shown in Fig. 1a, the Fourier transform of EXAFS (FT-EXAFS) spectrum of Mo/SiO2 exhibits well-resolved peaks corresponding to the neighboring oxygen atoms (MoO and MoO) at ca. 0.8–2.0 Å (without phase-shift correction), while an additional peak assignable to the MoOMo bond was not observed at ca. 3.0 Å [30]. The results of curve-fitting analysis of FT-EXAFS spectrum of Mo/SiO2 demonstrate that the majority of Mo6+-oxide has tetrahedral coordination with two short MoO double bonds (bond length (R) = 1.66 Å, coordination number (CN) = 2.1) and two long MoO single bonds (R = 1.89 Å, CN = 2.1). The results suggest that the Mo6+-oxide component within Mo/SiO2 exists predominantly in a tetrahedrally coordinated state. Similarly, XAFS analysis for V/SiO2 and Cr/SiO2 was used to explore the local structures of the V5+- and Cr6+-oxide moieties incorporated within SiO2. The V K-edge XANES and FT-EXAFS spectra of these components are displayed in Fig. 1B and b, respectively. The XANES spectrum of V/SiO2, containing a sharp pre-edge peak assigned to the 1s–3d transition of V5+-oxide, is similar to that of vanadium(V) triisopropoxide (data not shown) used as a reference for a V5+-oxide species with tetrahedral coordination [31]. This finding indicates that highly distorted and tetrahedrally coordinated V5+-oxide moieties can be incorporated within SiO2[32]. Moreover, the results of curve-fitting analysis of the FT-EXAFS spectrum of V/SiO2 demonstrate that V5+-oxide has highly distorted tetrahedral coordination with a shorter VO double bond (R = 1.53 Å, CN = 0.90) and three longer VO single bonds (R = 1.75 Å, CN = 3.0) [33]. The respective Cr K-edge XANES and FT-EXAFS spectra of Cr/SiO2 are displayed

in Fig. 1C and c. The XANES spectrum contains an intense and characteristic pre-edge peak attributable to the 1s–3d transition of Cr6+-oxide, indicating that Cr/SiO2 contains Cr6+-oxide moieties with tetrahedral coordination [34,35]. Furthermore, observations made in curve-fitting analysis of the FT-EXAFS spectrum reveal that the Cr6+-oxide species has a highly distorted, tetrahedral coordination with two shorter CrO double bonds (R = 1.59 Å, CN = 2.0) and two longer CrO single bonds (R = 1.85 Å, CN = 2.1) [21]. The results suggest that the three metal–oxide moieties (Mo, V, and Cr) incorporated within SiO2 exist in isolated and tetrahedrally coordinated states.

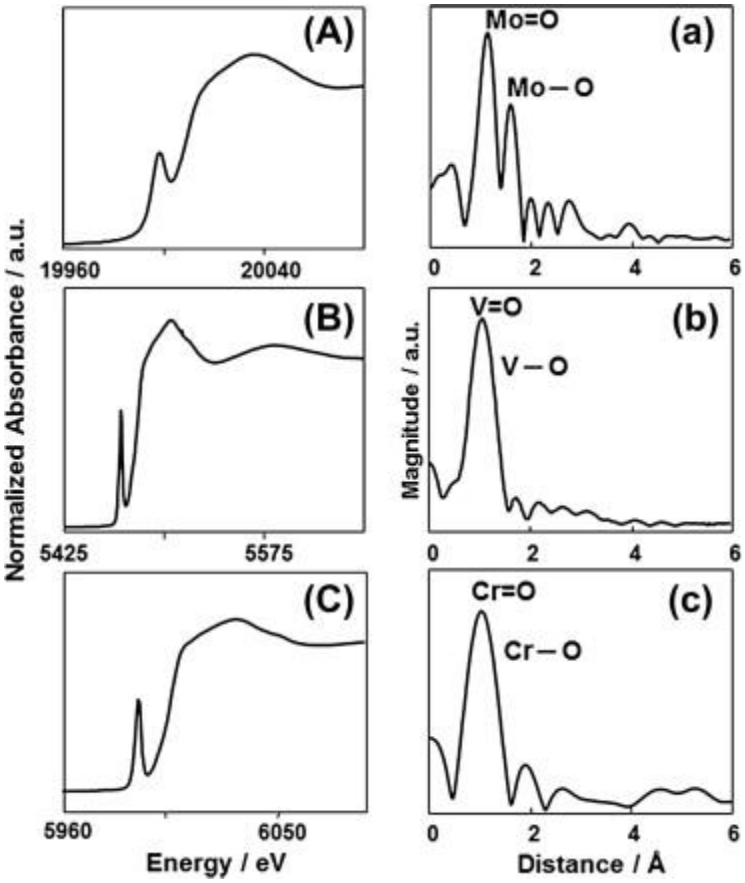

Fig. 1. (A–C) XANES and (a–c) FT-EXAFS spectra of (A and a) Mo/SiO2, (B and b) V/SiO2, and (C and c) Cr/SiO2.

To corroborate the assigned coordination states of the metal–oxide moieties incorporated within SiO2, UV–vis and photoluminescence spectra of M/SiO2 (MMo, V, and Cr) were conducted, as shown in Fig. 2. The diffuse reflectance UV–vis spectra contain characteristic peaks assignable to ligand-to-metal charge-transfer (LMCT) transitions from O2− to Mn+ (n = 5 or 6) ions in their tetrahedral geometry (Mo6+: 240 and 280 nm, V5+: 260 nm, Cr6+: 240, 350, and 460 nm) [21,30,36,37]. Importantly, typical absorption bands associated with aggregated metal–oxide species are not observed. This finding shows that metal–oxide moieties within M/SiO2 exist in tetrahedrally coordinated states and that no aggregated metal–oxide clusters are present, a finding that is in accord with the results obtained by using XAFS measurements. In the photoluminescence spectra of M/SiO2 (MMo, V, and Cr), observable emission bands occur at ca. 450 (Mo), 500 (V), and 630 (Cr) nm. The emission peaks are assignable to radioactive decay from charge-transfer-excited triplet states of tetrahedrally coordinated metal–oxide moieties in the manner described as follows [38–42].

(1)

Mo6+O2-⇄hv′hv[Mo5+O-]∗(Mo/SiO2)

(2)

V5+O2-⇄hv′hv[V4+O-]∗(V/SiO2)

(3)

Cr6+O2-⇄hv′hv[Cr5+O-]∗(Cr/SiO2)

Furthermore, the positions of emission bands are hardly changed when the excitation wavelength is varied (data not shown), suggesting that photoluminescence takes place in each case from only one type of the tetrahedral and isolated metal oxide moiety. The combined results coming from XAFS, UV–vis, and photoluminescence measurements reveal that single-site transition metal oxide moieties are incorporated with tetrahedral geometries within M/SiO2 (MMo, V, and Cr).

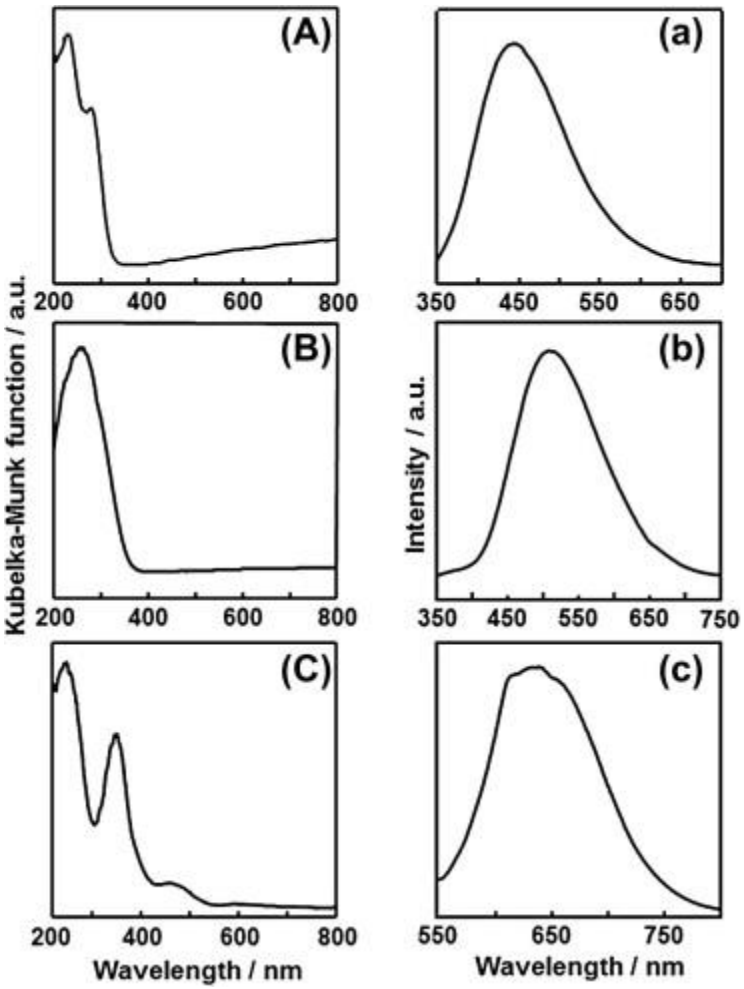

Fig. 2. (A–C) Diffuse reflectance UV–vis spectra and (a–c) photoluminescence spectra of (A and a) Mo/SiO2, (B and b) V/SiO2, and (C and c) Cr/SiO2. Photoluminescence measurement conditions: measurement temperature, 298 K; Excitation, λex = 300 nm (Mo, V) and 280 nm (Cr).

3.2. Photocatalytic reactions

Photocatalytic activities of M/SiO2 (MMo, V, and Cr) for NO (28 μmol) reduction with CO (28 μmol) under UV-light irradiation at 293 K were investigated. Fig. 3A–C shows the changes occurring in the amounts of gases as a function of reaction time (t), and the amounts of gases after 3 h of UV-light irradiation were summarized in Table 1. As can be seen in Fig. 3A, at the initial stage (t < 1 h), N2O and CO2 are produced in

nearly invariant ratios when Mo/SiO2 is employed as the photocatalyst. However, after 1-h irradiation, the amount of produced N2O begins to decrease in concert with the formation of N2. These results show that NO is initially reduced to form N2O, which is then converted to N2 (see reactions 1, 2).

2NO+CO→N2O+CO2reaction(1)

N2O+CO→N2+CO2reaction(2)

It should be noted that the second step in this process takes place only after the concentration of NO has significantly decreased. Different observations are made while monitoring the process catalyzed by V/SiO2 (Fig. 3B). Specifically, in the initial stage of the reaction (t < 1 h), NO is reduced to generate N2O accompanied by stoichiometric formation of CO2 (reaction (1)). However, the produced N2O is not converted to N2, even after prolonged irradiation, showing that V/SiO2 does not promote reaction (2). In contrast, almost no N2O and N2 are formed and only a small amount of CO2 is generated when Cr/SiO2 is utilized as the photocatalyst. This observation indicates that Cr/SiO2 is not an active photocatalyst for reduction of NO with CO. In an effort to elucidate the detailed reaction mechanism which accounts for the different photocatalytic performances of three kinds of M/SiO2 (MMo, V, and Cr), FT-IR measurement was performed, which is one of the most powerful and useful methods in the investigation of adsorption states as well as the reactivity of adsorbed molecules on catalytically active sites.

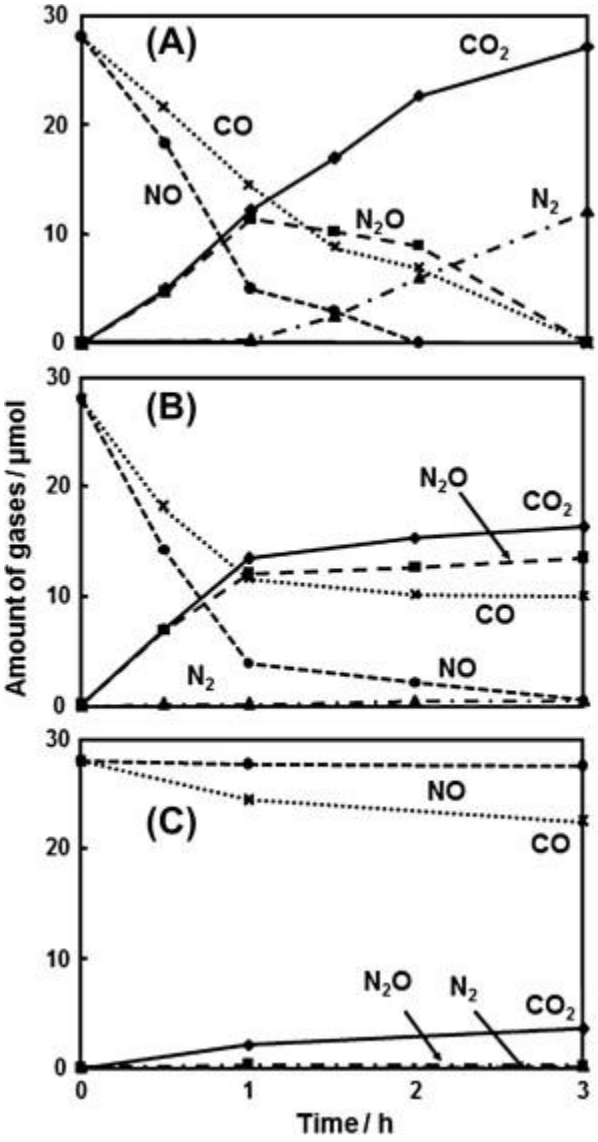

Fig. 3. Reaction time profiles of the photocatalytic reduction of NO with CO under UV-light irradiation over (A) Mo/SiO2, (B) V/SiO2, and (C) Cr/SiO2 at 298 K.

Table 1. The amounts of gases after 3 h of UV-light irradiation for the photocatalytic reduction of NO with CO over Mo/SiO_2, V/SiO_2, and Cr/SiO_2 at 298 K.

Catalyst	Amount of gas/μmol				
	CO	CO_2	NO	N_2O	N_2
Mo/SiO_2	0	27.1	0	0	12.0
V/SiO_2	10.0	16.2	0.4	13.4	0.4
Cr/SiO_2	22.6	3.7	27.6	0.1	0.1

3.3. Clarification of reaction mechanisms by using in situ FT-IR studies

3.3.1. In situ FT-IR monitoring of the process promoted by Mo/SiO2

FT-IR spectra of Mo/SiO2, which promotes photocatalytic reduction of NO with CO, in the presence of various gas combinations, were recorded. Fig. 4A and B shows the effects of the presence of NO and N2O, respectively, on CO adsorbed on Mo/SiO2 in the dark. The spectra were recorded following UV irradiation of Mo/SiO2 in the presence of CO, and addition of NO (0.3 kPa) or N2O (0.3 kPa) in the dark. Before addition of NO or N2O, FT-IR peaks due to the dicarbonyl (Mo4+(CO)2; 2127 and 2077 cm−1) and monocarbonyl (Mo4+(CO); 2043 cm−1) species were observed (Fig. 4A and a, and B and a') [43], indicating that Mo6+-oxide is photo-reduced by CO to form Mo4+-oxide–carbonyl species. This process occurs via a route involving excitation of Mo6+-oxide on Mo/SiO2 to form the corresponding charge-transfer-excited triplet state ([Mo5+O−]*) that reacts with CO to form Mo4+-oxide–carbonyl species accompanied by the generation of CO2[44]. Then, the reactivity of Mo4+-oxide–carbonyl species toward NO was investigated, as shown in Fig. 4A. Three absorption bands associated with Mo4+-oxide–carbonyl species were completely disappeared by the addition of NO within 30 s, indicating the reaction of Mo4+-oxide–carbonyl species with NO. In fact, the adsorption of NO on Mo/SiO2 was confirmed after NO addition onto Mo4+-oxide–carbonyl species. Fig. 5 shows the effect of the addition of NO on FT-IR spectrum in the N–O stretching region of the photo-reduced Mo/SiO2. Here, FT-IR monitoring of the process, involving irradiation of Mo/SiO2 in the presence of CO followed by the introduction of various pressures of NO in the dark, shows that addition of NO causes the appearance of a band at 1718 cm−1 assigned to the NO stretching vibration of a Mo4+(NO) species [45] whose intensity is directly dependent on the NO pressure. Moreover, the addition of excess NO (>5.0 Pa) leads to a decrease in the intensity of the peak at 1718 cm−1, indicating that gaseous NO reacts with Mo4+(NO) to form the original Mo6+-oxide species accompanied by production of N2O. In fact, the formation of N2O can be detected by using GC analysis.

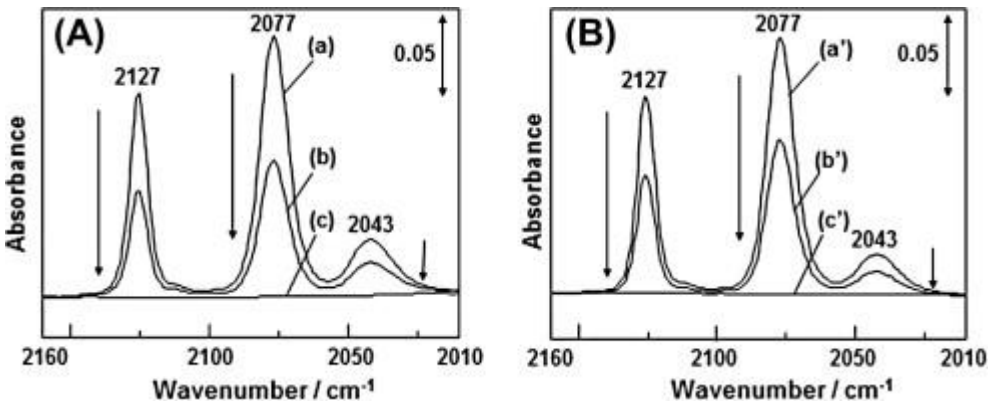

Fig. 4. Effects of (A) NO (0.3 kPa) and (B) N2O (0.3 kPa) addition in the dark on the FT-IR spectra of Mo/SiO2 photo-reduced by CO. Mo4+-oxide–carbonyl species was formed by UV-light irradiation in the presence of CO (0.6 kPa) ((a), (a')),

and then, NO or N2O was added. (A): (b) 10 s, (c) 30 s after NO addition. (B): (b′) 1 min, (c′) 3 min after N2O addition.

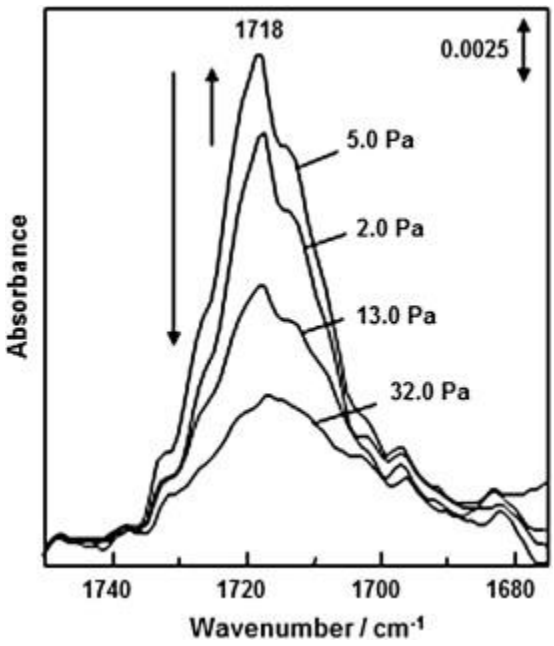

Fig. 5. Effect of the addition of NO on the FT-IR spectra of NO adsorbed on Mo/SiO2, which is photo-reduced by CO. NO was added after Mo4+-oxide–carbonyl species was formed by UV-light irradiation in the presence of CO (0.6 kPa).

The reaction of the Mo4+-oxide–carbonyl species with N2O was monitored next by using FT-IR (Fig. 4B). The intensities of characteristic FT-IR bands associated with Mo4+(CO)2 and Mo4+(CO) species were observed to decrease when N2O (0.3 kPa) was added in the dark. However, the rate of decrease in the intensities of these peaks (complete disappearance after 3 min) is lower than that caused by the addition of NO.

Based on these results, a possible reaction mechanism for the photocatalytic reduction of NO with CO catalyzed by Mo/SiO2 is proposed and shown in Scheme 1. In this process, the tetrahedrally coordinated Mo6+-oxide species is transformed by UV irradiation to the corresponding charge-transfer-excited triplet state, which reacts with CO to form the Mo4+-oxide–carbonyl species. The Mo4+-oxide–carbonyl species is then oxidized by NO in the dark to produce the original Mo6+-oxide species along with N2O. Following almost complete consumption of NO, the remaining Mo4+-carbonyl species reacts with N2O in the dark to generate the original Mo6+-oxide and N2.

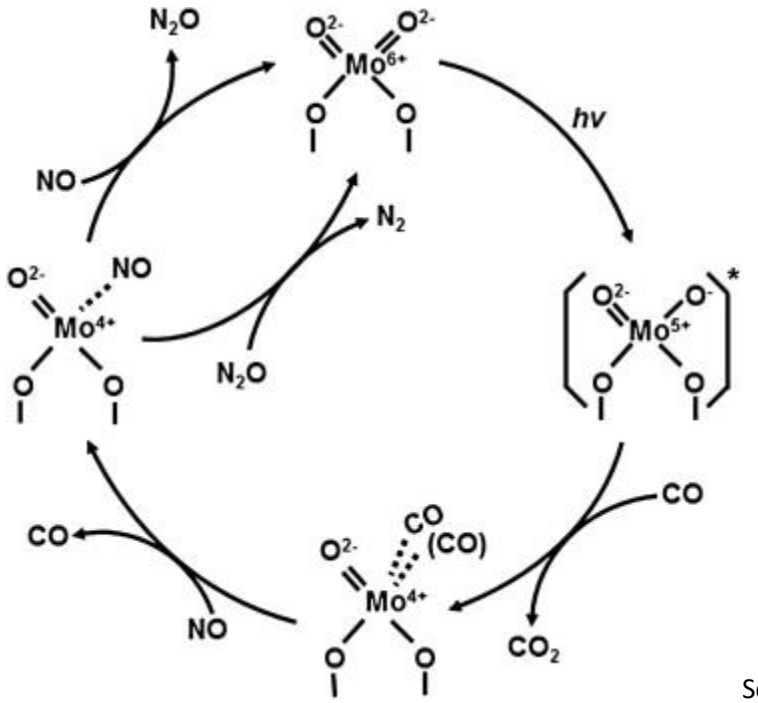

Scheme 1. Catalytic cycles for the photocatalytic reduction of NO with CO on Mo/SiO2 under UV-light irradiation.

3.3.2. In situ FT-IR monitoring of the process promoted by V/SiO2

A similar FT-IR study was conducted to explore the process catalyzed by V/SiO2. As shown in Fig. 3B, the photocatalytic reduction of NO with CO (reaction (1)) proceeds on V/SiO2, leading to the production of N2O without followed by reaction (2), that is, further reduction of N2O into N2 does not proceed. Fig. 6 shows the time-dependent changes of bands in the FT-IR spectrum of V/SiO2 under UV-light irradiation in the presence of CO (0.6 kPa). The absorption bands assignable to the monocarbonyl (V3+(CO); 2185 and 2169 cm−1) species appeared by UV irradiation of V/SiO2 in the presence of CO, indicating that V5+-oxide species are photo-reduced to V3+-oxide–carbonyl species by CO [46]. This result suggests that the charge-transfer-excited triplet state, that is, [V4+O−]* is reduced to form V3+-oxide–carbonyl species (V3+(CO)) and CO2 via reaction with CO [44].

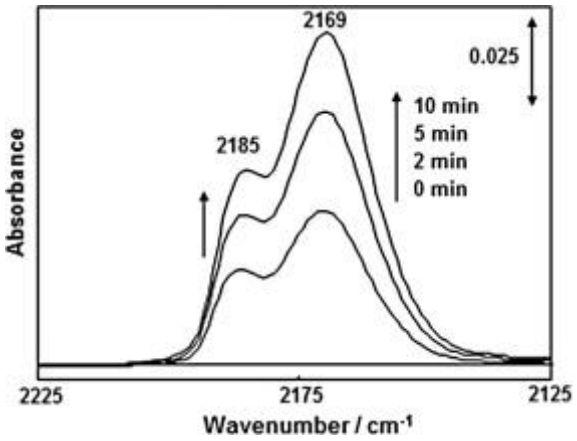

Fig. 6. FT-IR spectra observed under UV-light irradiation for 10 min on V/SiO2 in the presence of CO (0.6 kPa).

FT-IR measurements were performed under various NO pressures in order to investigate the reactivity of V3+(CO) with NO. Fig. 7 shows FT-IR spectra of V/SiO2, following photo-reduction in the presence of CO and addition of various pressures of NO. The observations indicate that under lower NO pressure (0–3.6 Pa) conditions a characteristic FT-IR peak at 1717 cm−1, assigned to adsorbed NO on V3+-oxide species

(V3+(NO)), appears (Fig. 7A) [47], suggesting that V3+(CO) reacts with NO to form V3+(NO). Addition of larger amounts of NO (3.6–273.2 Pa) leads to a decrease in the intensity of this band (Fig. 7B). This result clearly demonstrates that V3+(NO) species reacts with NO to form the original V5+-oxide species (V5+O2−) and N2O (verified by using GC analysis). However, in contrast to the process promoted by Mo/SiO2, V/SiO2 does not catalyze further reaction of N2O. In fact, as shown in Fig. 8, the FT-IR band at 1717 cm−1, attributed to V3+(NO), remains nearly unchanged following the addition of N2O even under UV-light irradiation conditions. Thus, it appears that V3+(NO) is sufficiently stable to prohibit its reoxidation of V3+-oxide species by N2O, and hence, reduction of N2O to form N2 does not take place. The observations suggest that photocatalytic reduction of NO with CO on V/SiO2 proceeds through the catalytic cycle displayed in Scheme 2, in which the tetrahedrally coordinated V5+-oxide species is photo-excited to produce its charge-transfer-excited triplet state that reacts with CO to form CO2 and V3+-carbonyl species (V3+(CO)). This is followed by oxidation of the V3+(CO) species to form the original V5+-oxide species and N2O. However, further reduction of N2O to generate N2 does not occur because of the formation of NO-adsorbed V3+-oxide species (V3+(NO)) which is stable enough to prohibit the reoxidation of V3+-oxide species by N2O.

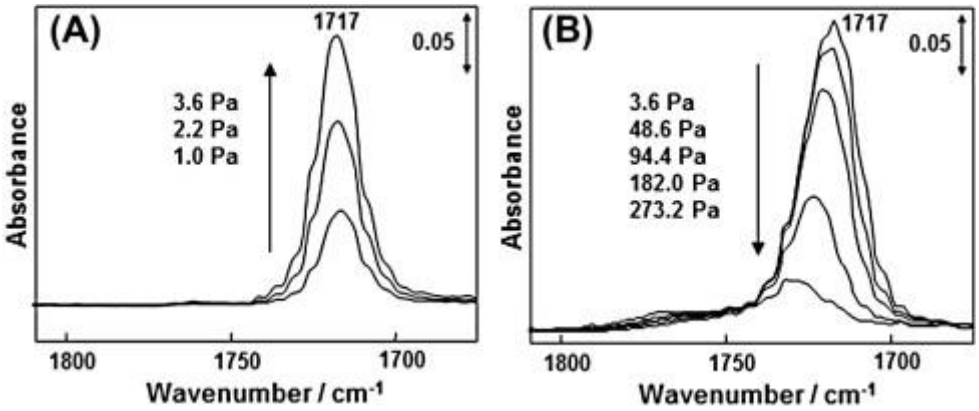

Fig. 7. Effect of NO pressure on the FT-IR spectra of NO adsorbed on V/SiO2 which is photo-reduced by CO (A) in the low-pressure region (NO pressure: 0–3.6 Pa) and (B) in the high-pressure region (NO pressure: 3.6–273.2 Pa). NO was added after V3+-oxide–carbonyl species was formed by UV-light irradiation in the presence of CO (0.6 kPa).

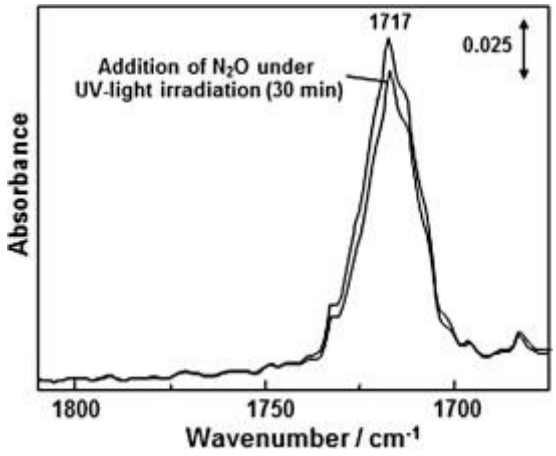

Fig. 8. Effect of the addition of N2O (0.3 kPa) under UV-light irradiation on the FT-IR spectra of NO adsorbed on V/SiO2 which is photo-reduced by CO. V3+(NO) species (1717 cm−1) was formed by UV-light irradiation in the presence of CO (0.6 kPa) and following addition of NO (0.3 Pa). N2O was then added and UV-light irradiation was carried out for 30 min.

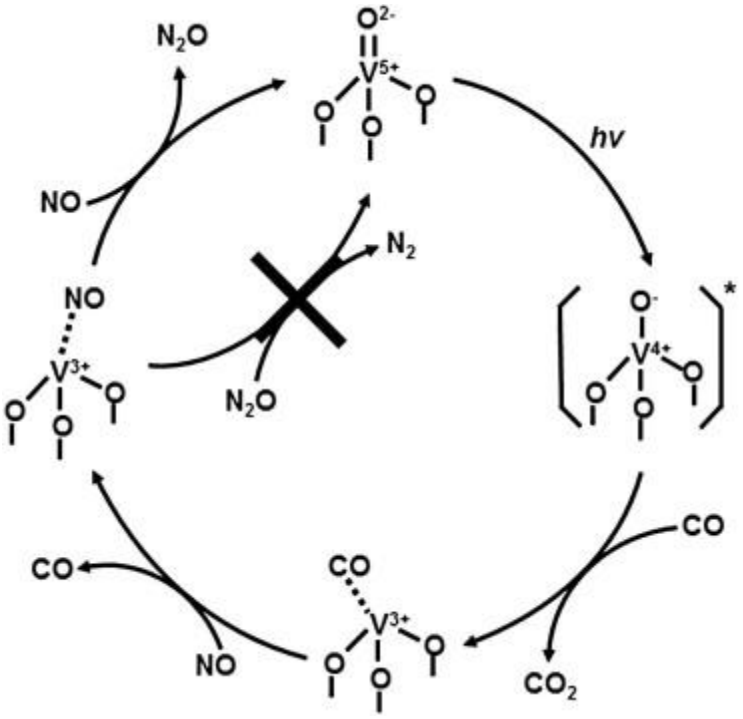

Scheme 2. Catalytic cycles for the photocatalytic reduction of NO with CO on V/SiO2 under UV-light irradiation.

3.3.3. In situ FT-IR monitoring of the process promoted by Cr/SiO2

Finally, the FT-IR spectroscopic method was employed to determine the reason why Cr/SiO2 does not promote photocatalytic reduction of NO with CO. The time-dependent changes taking place in the FT-IR spectrum when Cr/SiO2 is UV-irradiated in the presence of CO (6.7 kPa) are shown in Fig. 9. As is the case with the Mo/SiO2- and V/SiO2-catalyzed processes, the appearance of the absorption bands assigned to monocarbonyl species (Cr2+(CO): 2178 and 2188 cm−1) [48] is observed by UV-light irradiation of Cr/SiO2 in the presence of CO. The appearance of these peaks indicates that CO reacts with the charge-transfer-excited triplet state ([Cr5+O−]*), leading to the formation of Cr2+-oxide–carbonyl species and CO2. In addition, the formation of CO2 in this process is detected by using GC analysis. Possible reactions taking place between NO and the Cr2+-oxide–carbonyl species were explored by monitoring the effects of addition of a high pressure of NO (5.2 kPa) by using FT-IR. As displayed in Fig. 10a, the well-resolved peak at 2180 cm−1 corresponding to CO stretching in Cr2+(CO)(NO)2 species remains even after the addition of a high pressure of NO [49]. In addition, strong FT-IR peaks associated with typical NO stretching vibrations of Cr2+(CO)(NO)2 species are observed at 1875 and 1755 cm−1[50] in addition to the CO stretching band (2180 cm−1). The intensities of these strong peaks (2180, 1875, and 1755 cm−1) remain nearly unchanged even after 1 h in the dark, showing that the Cr2+(CO)(NO)2 species is stable even at ambient temperatures. It should be noted that the complete evacuation of the reaction system leads to a decrease in the intensities of FT-IR peaks at 1875 and 1755 cm−1 accompanied by a strong increase in the peaks at 1854 and 1742 cm−1 (Fig. 10b). These results show that Cr2+(CO)(NO)2 species is transformed to Cr2+(NO)2 species (1854 and 1742 cm−1) that is also stable at ambient temperatures [50].

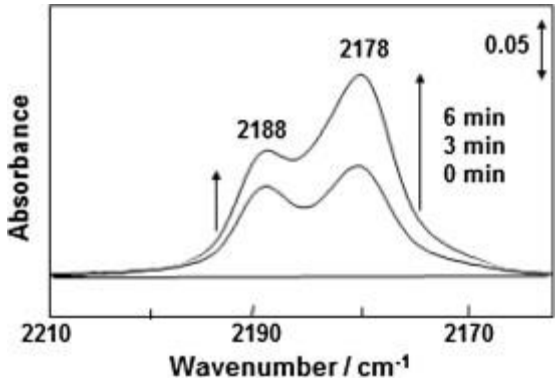

Fig. 9. FT-IR spectra observed under UV-light irradiation for 10 min on Cr/SiO2 in the presence of CO (6.7 kPa).

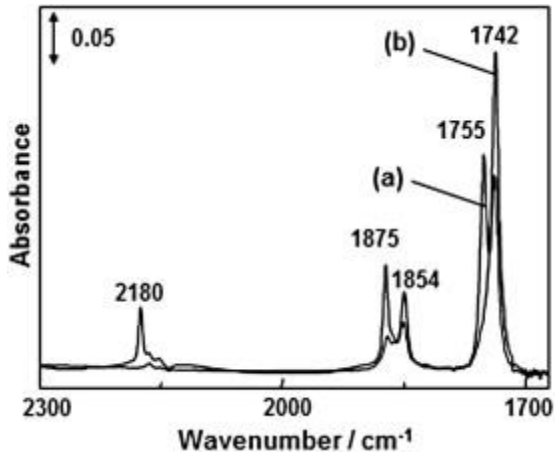

Fig. 10. FT-IR spectrum observed (a) after the addition of high-pressure NO (5.2 kPa) on Cr/SiO2 which is photo-reduced by CO and (b) the effect of following evacuation treatment. NO (5.2 kPa) was added after Cr2+-oxide–carbonyl species was formed by UV-light irradiation in the presence of CO (0.6 kPa).

The combined results clearly show that Cr2+-oxide–carbonyl species react with NO to form stable Cr2+(CO)(NO)2 species (or Cr2+(NO)2 species in the absence of gaseous CO) but that oxidation of Cr2+ to form N2O and N2 does not take place. Thus, the reaction mechanism for the photocatalytic reduction of NO with CO catalyzed by Cr/SiO2, shown in Scheme 3, appears to be plausible. In this pathway, the tetrahedrally coordinated Cr6+-oxide species is photo-excited into its charge-transfer-excited triplet state and reacts with CO to form the Cr2+-oxide–carbonyl species. Then, the Cr2+-oxide–carbonyl species react with NO to form Cr2+(CO)(NO)2 species, which is not oxidized by NO. Consequently, photocatalytic reduction of NO with CO over Cr/SiO2 does not proceed.

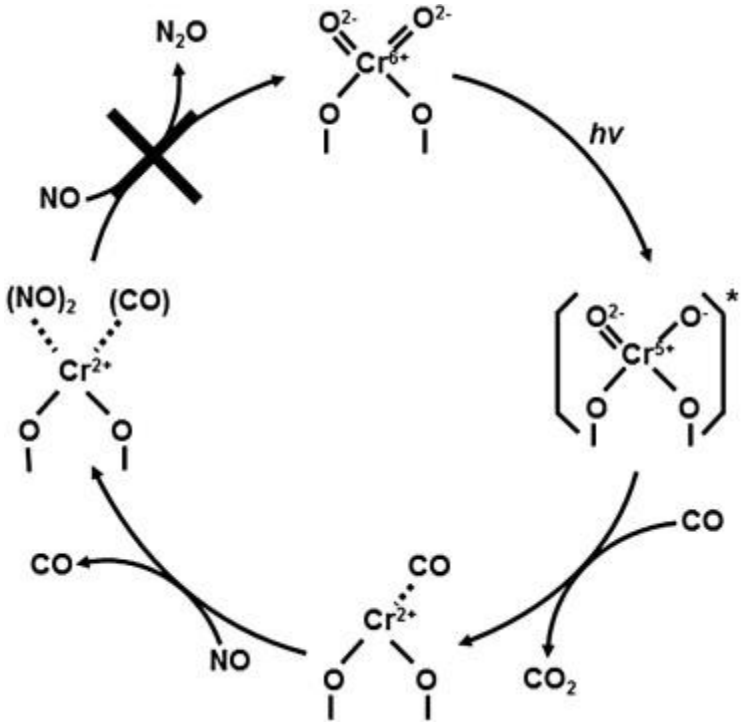

Scheme 3. Catalytic cycles for the photocatalytic reduction of NO with CO on Cr/SiO2 under UV-light irradiation.

As a whole, the results of photocatalytic reduction of NO with CO over various single-site photocatalysts (M/SiO2: MMo, V, and Cr), summarized in Scheme 4, show that the single-site photocatalysts exhibit different activities in this process. Specifically, photocatalytic reduction of NO over Mo/SiO2 proceeds efficiently to produce N2 via N2O as an intermediate product. In contrast, V/SiO2 promotes NO reduction reaction, leading to the production of N2O without accompanying reduction to produce N2. Finally, neither N2 nor N2O and only a small amount of CO2 are observed to form when Cr/SiO2 is used as the photocatalyst.

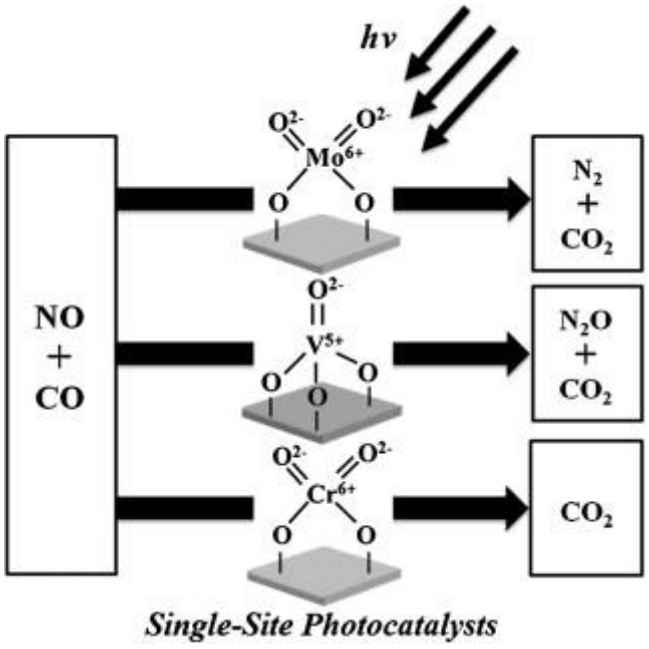

Scheme 4. Schematic summary of the photocatalytic reduction of NO with CO on various single-site photocatalysts (M/SiO2: MMo, V, and Cr) under UV-light irradiation.

4. Conclusion

In this effort, various transition metal oxide-incorporating SiO_2 (Mo, V, and Cr/SiO_2) were prepared by using an impregnation method. The results of XAFS, UV–vis, and photoluminescence measurements reveal that metal oxide moieties in M/SiO_2 exist in isolated and tetrahedrally coordinated states. The activities of these photocatalysts for photocatalytic reduction of NO with CO were investigated by employing FT-IR spectroscopy. Mo/SiO_2 exhibits high activity in the photocatalytic reduction of NO with CO under UV-light irradiation, leading to the production of N_2 and CO_2. On the contrary, the reactions did not proceed efficiently over V and Cr/SiO_2. NO was photocatalytically reduced into N_2O in the presence of V/SiO_2, while further reduction of N_2O into N_2 could not proceed due to the formation of unreactive NO-adsorbed V^{3+}-oxide species which is stable enough to prohibit the reoxidation of V^{3+}-oxide species by N_2O. It was also found that Cr/SiO_2 does not promote photocatalytic reduction of NO, because the reoxidation to produce the original Cr^{6+} species hardly occurs due to the unreactive species generated by the adsorption of NO onto Cr^{2+}-oxide species. These findings will contribute to the deep understanding of unique photocatalytic activity of single-site photocatalysts.

Acknowledgment

The present work is supported by a Grant-in-Aid for Scientific Research (KAKENHI) from Ministry of Education, Culture, Sports, Science and Technology of Japan (No. 21550192).

References

[1]
M. Matsuoka, M. Anpo
J. Photochem. Photobiol. C, 3 (2003), p. 225
[2]
S.S. Arbuj, R.R. Hawaldar, S. Varma, S.B. Waghmode1, B.N. Wani
Sci. Adv. Mater., 4 (2012), p. 568
[3]
H.G. Oliveira, B.C. Fitzmorris, C. Longo, J.Z. Zhang
Sci. Adv. Mater., 4 (2012), p. 673
[4]
M. Kitano, K. Iyatani, E. Afsin, Y. Horiuchi, M. Takeuchi, S.H. Cho, M. Matsuoka, M. Anpo
Res. Chem. Intermed., 38 (2012), p. 1249
[5]
T.T. Lea, M.S. Akhtara, D.M. Parka, J.C. Leec, O.B. Yang
Appl. Catal., B Environ., 111–112 (2012), p. 397
[6]
M.A. Khan, M.S. Akhtar, S.I. Woo, O.B. Yang
Catal. Commun., 10 (2008), p. 1
[7]
R. Tode, A. Ebrahimi, S. Fukumoto, K. Iyatani, M. Takeuchi, M. Matsuoka, M. Anpo
Catal. Lett., 135 (2010), p. 10
[8]
P. Ji, M. Takeuchi, T.-M. Cuong, J. Zhang, M. Matsuoka, M. Anpo
Res. Chem. Intermed., 36 (2010), p. 327
[9]
M. Takeuchi, M. Matsuoka, M. Anpo
Res. Chem. Intermed., 38 (2012), p. 1261
[10]
H. Yamashita, M. Harada, J. Misaka, M. Takeuchi, B. Neppolian, M. Anpo
Catal. Today, 84 (2003), p. 191
[11]

X. Zhao, H. Li, H.S. Wang, Z. Zhong
Sci. Adv. Mater., 3 (2011), p. 984
[12]
Z. Jin, G.T. Fei, X.Y. Hu, M. Wang, L.D. Zhang
J. Nanoeng. Nanomanuf., 2 (2012), p. 49
[13]
M. Takeuchi, J. Deguchi, S. Sakai, M. Anpo
Appl. Catal., B, 96 (2010), p. 218
[14]
M. Takeuchi, J. Deguchi, M. Hidaka, S. Sakai, K. Woo, P.P. Choi, J.K. Park, M. Anpo
Appl. Catal., B, 89 (2009), p. 406
[15]
M. Anpo, J.M. Thomas
Chem. Commun. (2006), p. 3273
[16]
H. Yamashita, K. Mori
Chem. Lett., 36 (2007), p. 348
[17]
T. Kamegawa, M. Matsuoka, M. Anpo
Res. Chem. Intermed., 34 (2008), p. 427
[18]
M. Anpo, Y. Kubokawa
Res. Chem. Intermed., 8 (1987), p. 105
[19]
M. Anpo, S.G. Zhang, S. Higashimoto, M. Matsuoka, H. Yamashita, Y. Ichihashi, Y. Matsumura, Y. Souma
J. Phys. Chem. B, 103 (1999), p. 9295
[20]
S. Takenaka, T. Tanaka, T. Funabiki, S. Yoshida
J. Chem. Soc., Faraday Trans., 94 (1998), p. 695
[21]
T. Kamegawa, J. Morishima, M. Matsuoka, J.M. Thomas, M. Anpo
J. Phys. Chem. C, 111 (2006), p. 1076
[22]
M. Matsuoka, T. Kamegawa, R. Takeuchi, M. Anpo
Catal. Today, 122 (2007), p. 39
[23]
A. Chaloulakou, I. Mavroidis, I. Gavriil
Atmos. Environ., 42 (2008), p. 454
[24]
M. Anpo, M. Matsuoka, H. Mishima, H. Yamashita
Res. Chem. Intermed., 23 (1997), p. 197
[25]
M. Haruta, S. Tsubota, T. Kobayashi, H. Kageyama, M.J. Genet, B. Delmon
J. Catal., 144 (1993), p. 175
[26]
K. Yokota, M. Fukui, T. Tanaka
Appl. Surf. Sci., 121 (1997), p. 273
[27]
T. Nakatsuji, T. Yamaguchi, N. Sato, H. Ohno
Appl. Catal., B, 85 (2008), p. 61
[28]
S. Higashimoto, Y. Hu, R. Tsumura, K. Iino, M. Matsuoka, H. Yamashita, Y.G. Shul, M. Che, M. Anpo
J. Catal., 235 (2005), p. 272

[29]
S. Bordiga, S. Coluccia, C. Lamberti, L. Marchese, A. Zecchina, F. Boscherini, F. Buffa, F. Genoni, G. Leofanti
J. Phys. Chem., 98 (1994), p. 4125
[30]
T. Kamegawa, R. Takeuchi, M. Matsuoka, M. Anpo
Catal. Today, 111 (2006), p. 248
[31]
J. Wong, F.W. Lytle, R.P. Messmer, D.H. Maylotte
Phys. Rev. B, 30 (1984), p. 5596
[32]
R. Rulkens, J.L. Male, K.W. Terry, B. Olthof, A. Khodakov, A.T. Bell, E. Iglesia, T.D. Tilley
Chem. Mater., 11 (1999), p. 2966
[33]
T. Tanaka, H. Yamashita, R. Tsuchitani, T. Funabiki, S. Yoshida
J. Chem. Soc. Faraday Trans., I (84) (1988), p. 2987
[34]
B.M. Weckhuysen, R.A. Schoonheydt, J.-M. Jehng, I.E. Wachs, S.J. Cho, R. Ryoo, S. Kijlstra, E. Poels
J. Chem. Soc., Faraday Trans., 91 (1995), p. 3245
[35]
L.A. Grunes
Phys. Rev. B, 27 (1983), p. 2111
[36]
K.J. Chao, C.N. Wu, H. Chang, L.J. Lee, S.-f. Hu
J. Phys. Chem. B, 101 (1997), p. 6341
[37]
H. Yamashita, S. Ohshiro, K. Kida, K. Yoshizawa, M. Anpo
Res. Chem. Intermed., 29 (2003), p. 881
[38]
B. Shelimov, V. Dellarocca, G. Martra, S. Coluccia, M. Che
Catal. Lett., 87 (2003), p. 73
[39]
S. Dzwigaj, M. Matsuoka, R. Franck, M. Anpo, M. Che
J. Phys. Chem. B, 102 (1998), p. 6309
[40]
B. Fubini, G. Ghiotti, L. Stradella, E. Garrone, C. Morterra
J. Catal., 66 (1980), p. 200
[41]
R. Tsumura, S. Higashimoto, M. Matsuoka, H. Yamashita, M. Che, M. Anpo
Catal. Lett., 68 (2000), p. 101
[42]
S. Higashimoto, R. Tsumura, S.G. Zhang, M. Matsuoka, H. Yamashita, C. Louis, M. Che, M. Anpo
Chem. Lett., 4 (2000), p. 408
[43]
C.C. Williams, J.G. Ekerdt
J. Phys. Chem., 97 (1993), p. 6843
[44]
F. Amano, T. Yamaguchi, T. Tanaka
J. Phys. Chem. B, 110 (2005), p. 281
[45]
J.B. Peri
J. Phys. Chem., 86 (1982), p. 1615
[46]
T.V. Venkov, C. Hess, F.C. Jentoft

Langmuir, 23 (2006), p. 1768
[47]
E. Ivanova, K. Hadjiivanov, S. Dzwigaj, M. Che
Micropor. Mesopor. Mater., 89 (2006), p. 69
[48]
G. Ghiotti, E. Garrone, A. Zecchina
J. Mol. Catal., 46 (1988), p. 61
[49]
G. Spoto, S. Bordiga, E. Garrone, G. Ghiotti, A. Zecchina, G. Petrini, G. Leofanti
J. Mol. Catal., 74 (1992), p. 175
[50]
A. Zecchina, G. Spoto, G. Ghiotti, E. Garrone
J. Mol. Catal., 86 (1994), p. 423